

1
2
3
4
5
6
7
8
9
10
11
12
13
14
15
16
17
18
19
20
21
22
23
24
25
26
27
28
29
30
31
32
33
34
35
36
37
38

**Temporal Coding of Taste in the
Parabrachial Nucleus of the Pons of the Rat**

Andrew M. Rosen¹, Jonathan D. Victor² and Patricia M. Di Lorenzo^{1,3}

¹Department of Psychology, Binghamton University, Binghamton, NY

²Dept. of Neurology and Neuroscience, Weill Cornell Medical College, NY, NY

³To whom correspondence should be addressed
Dept. of Psychology
Box 6000
Binghamton University
Binghamton, NY 13902-6000
Ph: 607-777-2055
FAX: 607-777-4890
Email: diloren@binghamton.edu

39
40**ABSTRACT**

41 Recent studies have provided evidence that temporal coding contributes significantly to encoding
42 taste stimuli at the first central relay for taste, the nucleus of the solitary tract (NTS). However,
43 it is not known whether this coding mechanism is also used at the next synapse in the central
44 taste pathway, the parabrachial nucleus of the pons (PbN). In the present study,
45 electrophysiological responses to taste stimuli (sucrose, NaCl, HCl, and quinine) were recorded
46 from 44 cells in the PbN of anesthetized rats. In 29 cells, the contribution of the temporal
47 characteristics of the response to the discrimination of various taste qualities was assessed. A
48 family of metrics that quantifies the similarity of two spike trains in terms of spike count and
49 spike timing was used. Results showed that spike timing in 14 PbN cells (48%) conveyed a
50 significant amount of information about taste quality, beyond what could be conveyed by spike
51 count alone. In another 14 cells (48%), the rate envelope (time course) of the response
52 contributed significantly more information than spike count alone. Across cells there was a
53 significant correlation ($r = 0.51$, $P < 0.01$) between breadth of tuning and the proportion of
54 information conveyed by temporal dynamics. Comparison with previous data from the NTS (Di
55 Lorenzo and Victor 2003, 2006) showed that temporal coding in the NTS occurred in a similar
56 proportion of cells and contributed a similar fraction of the total information at the same average
57 level of temporal precision, even though trial-to-trial variability was higher in the PbN than in
58 the NTS. These data suggest that information about taste quality conveyed by the temporal
59 characteristics of evoked responses is transmitted with high fidelity from the NTS to the PbN.

60 **Keywords:** taste, gustatory, temporal coding, parabrachial pons, brainstem, neural coding

61 **Running Head:** Temporal coding of taste in the pons

INTRODUCTION

62
63
64
65
66
67
68
69
70
71
72
73
74
75
76
77
78
79
80
81
82
83
84

In studies of neural coding of sensory stimuli, it is not uncommon for electrophysiological studies to focus on a single structure in the central pathway. In such cases the characterization of the sensory representation in one structure can provide a context with which to interpret neural coding in structures further upstream. That is, if the same form of neural coding is identified in multiple structures in a neural pathway, the argument that these mechanisms are in fact an essential system-wide method for communicating information is substantially strengthened. Here we present a study of information processing of taste stimuli in the parabrachial nucleus of the pons (PbN), the second relay in the central gustatory pathway, and compare it to what is known about neural processing of taste in the nucleus of the solitary tract (NTS), the primary source of taste-related information to the PbN. The focus of our investigation is on the analysis of the temporal characteristics of taste responses, defined as temporal coding.

Information about stimuli of particular taste qualities (sweet, sour, salt, bitter and perhaps umami) conveyed by peripheral nerves converges onto multisensitive cells in the NTS. The broad sensitivity of the majority of NTS cells often makes spike count an ambiguous signal for identification of taste quality. Under those conditions, a method of encoding that utilizes the temporal features of the response for stimulus discrimination may be better suited to the task. Previous studies have shown that approximately half of NTS cells utilize temporal coding in the representation of taste (Di Lorenzo and Victor 2003). Further, temporal coding can disambiguate taste stimuli of similar quality but different chemical composition (Roussin et al. 2008) as well as individual taste qualities when presented at different concentrations (Chen et al., in press).

85 Moreover, the temporal characteristics of taste responses contribute information about the
86 components of binary mixtures of tastants of different qualities, especially in cells that are
87 broadly tuned across taste qualities (Di Lorenzo et al. 2009).

88 In the rodent gustatory system, the main target of the NTS is the parabrachial nucleus of the
89 pons (PbN). The neural circuitry that interconnects the NTS and PbN is complex and involves
90 subnuclei with connections to areas controlling orofacial and ingestive behaviors as well as
91 reward. In both rat and hamster, the rostral central NTS, the subnucleus that receives most of the
92 afferent input from peripheral nerves innervating taste buds (Whitehead 1988; Lundy and
93 Norgren 2004), sends the majority of its output to the waist area of the PbN. This area includes
94 the central medial and ventral lateral nuclei and the cells that are scattered within the portion of
95 the brachium between them (Norgren 1978; Travers 1988). The waist area then sends a heavy
96 projection back to the ventral subnucleus of the NTS, which in turn sends projections to the
97 underlying medullary reticular formation, an area containing premotor circuits for taste-evoked
98 orofacial behaviors (Travers and Norgren 1983; Halsell et al. 1996; Karimnamazi and Travers
99 1998). There are also direct projections from the waist area to the medial reticular formation as
100 well as ascending projections to the thalamus, amygdala, hypothalamus and insular cortex
101 (reviewed in Lundy and Norgren 2004). Most of these forebrain connections are reciprocal,
102 suggesting a widely distributed and highly interactive circuit (see Katz et al. 2002; Simon et al.
103 2006). It is therefore an open question as to whether information about taste stimuli conveyed by
104 spike timing in the NTS would also be evident the PbN.

105 The purpose of the present study was to evaluate temporal coding of taste stimuli in the PbN
106 in the context of what is known about temporal coding in the NTS. Results show that temporal
107 coding contributes a significant proportion of the total information conveyed by taste-evoked

108 spike trains in the PbN. Further, temporal coding in the PbN occurs with the same prevalence
109 and with the same level of temporal precision as that found in the NTS even though trial-to-trial
110 variability in spike count increases. Collectively, these data support the idea that information
111 conveyed by the temporal characteristics of taste responses is preserved at the second synapse in
112 the central gustatory system.
113

114
115
116
117
118
119
120
121
122
123
124
125
126
127
128
129
130
131
132
133
134
135
136
137

MATERIALS AND METHODS

Subjects

Thirty-four male Sprague-Dawley rats (350-450 g) were used in this study. Rats were given unrestricted access to food and water and were paired housed with a 12 hour light-dark schedule. A plastic tube was placed in each cage to provide environmental stimulation. Animal care was in accord with the requirements of the Institutional Animal Care and Use Committee of Binghamton University.

Surgery

Prior to surgery, rats were anesthetized with urethane (1.5 g/kg, i.p., in two doses given 20 min apart). Supplemental injections of urethane (0.1 ml) were delivered as needed to maintain anesthesia. Robinul (glycopyrrolate), a peripheral anticholinergic agent (0.0004 g/kg, 10% in isotonic saline) was administered subcutaneously to facilitate breathing when necessary. Body temperature was maintained at 35-37° C during surgery with a rectal thermistor probe connected to a heating pad (FHC, Inc., Bowdoinham, ME).

Animals were tracheotomized to facilitate breathing during stimulus delivery. Their head was mounted in a stereotaxic instrument with upper incisor bar positioned 5 mm below the interaural line. Skin and fascia were removed and a nontraumatic head holder was secured to the skull with stainless steel screws and dental cement. This allowed better access to the mouth without the obstruction of the ear and tooth bars. The occipital bone and underlying meninges were removed and a small area of the posterior cerebellum was gently aspirated to provide access to the obex.

138

139 ***Taste stimuli and stimulus delivery***

140 Taste stimuli consisted of 0.1 M NaCl, 0.01 M HCl, 0.01 M quinine and 0.5 M sucrose.
141 These concentrations have been shown to elicit half-maximal potentials in the CT nerve of the
142 rat (Ganchrow and Erickson, 1970; Ogawa et al., 1974), and matched those used in our previous
143 studies of the NTS (Chen et al. in press; Di Lorenzo and Victor 2003, 2007; Di Lorenzo et al.
144 2009; Roussin et al. 2008). Taste stimuli were made from reagent-grade chemicals dissolved in
145 distilled water and were delivered at room temperature. The stimulus delivery system consisted
146 of stimulus-filled reservoirs pressurized with compressed air and connected via polyethylene
147 tubing to perforated stainless steel tubes placed in the mouth. Tastant delivery was controlled by
148 computer activation of a solenoid valve interposed between the reservoir and the tongue.
149 Tastants were delivered at a flow rate of 5 ml/s. The taste solution bathed the whole mouth; this
150 was verified by application of methylene blue through the system. Each stimulus trial consisted
151 of 10 sec spontaneous activity, 10 sec of pre-stimulus distilled water, 5 sec of tastant, 5 sec pause
152 and 20 sec of a distilled water rinse. The inter-trial interval was 2 min. Stimuli were presented
153 in repeated trials for as long as the cell remained well isolated. For any given stimulus, all other
154 stimuli were presented before it was repeated.

155

156 ***Electrophysiological recording and testing***

157 Electrophysiological recordings were performed with etched tungsten microelectrodes
158 (18–20 M Ω , 1 V at 1 kHz, FHC, Inc., Bowdoinham, ME). The electrode was lowered through
159 the cerebellum above the pons located 5.4 mm anterior and 1.8 mm lateral to the obex and 5-6
160 mm below the cerebellar surface. Signals were amplified (Model P511, Grass Technologies,

161 West Warwick, RI) and fed to a computer. The activity was digitized with an analogue-to-digital
162 interface (Model 1401, Cambridge Electronic Designs, Cambridge, UK) and was processed with
163 Spike2 software (Cambridge Electronic Designs, Cambridge, UK). Single cells were identified
164 by periodically delivering a 0.1 M NaCl solution followed by a water rinse as the electrode was
165 slowly lowered through the brain. Once a background response to NaCl was detected, every
166 well-isolated cell thereafter was tested with all four taste stimuli. Cell isolation was based on the
167 consistency of the waveform shape using template matching and principal component analysis.
168 A signal to noise ratio of 3:1 was required for cell isolation. Isolated cells were tested with the
169 exemplars of the four basic taste qualities yielding the “response profile” of the cell, defined as
170 the relative response rates across tastants. The cell was tested for as long as it remained isolated
171 allowing for multiple presentations of the same stimulus. Spike timing (1 ms precision) was
172 calculated with respect to the onset of each stimulus delivery.

173

174 ***Data analysis***

175 The magnitude of response to a given tastant was defined as the mean firing rate (spike
176 per second; sps) during the first 2 sec of tastant delivery minus the average firing rate (sps)
177 during the 5 sec of water delivery immediately preceding taste stimulus onset. A taste response
178 was considered to be significant if it was 2.5 standard deviations greater than the average
179 spontaneous firing rate. The breadth of tuning of taste-responsive cells was calculated with the
180 Uncertainty measure (Smith and Travers 1979). The formula for Uncertainty was

181

182

$$U = -k \sum P_i (\log P_i)$$

183

184 where k (scaling factor) = 1.66 for four stimuli and P_i is the proportion of response to stimulus i

185 relative to the summed responses to all four stimuli. Values ranged from 0 to 1.0 with 0

186 corresponding to a cell responsive to only one stimulus and 1.0 corresponding to a cell equally
187 responsive to all four stimuli. The absolute values of inhibitory taste responses were used for the
188 analysis of breadth of tuning with the Uncertainty measure (see Smith and Travers 1979 for a
189 discussion). We labeled this measure “*U*” for Uncertainty rather than “*H*” as in Smith and
190 Travers’ article (1979) to avoid confusion with the “*H*” value that indicated information
191 calculated in the analyses of temporal coding, described below.

192

193 *Metric space analyses of temporal patterns of response*

194 The analytical methods described in Victor and Purpura (1996, 1997) provide a rigorous
195 way to determine whether stimulus evoked spike trains have the potential to carry information
196 about the taste stimuli. A detailed description of this analysis as it has been applied to
197 electrophysiological recordings in the taste system has been published previously (Di Lorenzo
198 and Victor 2003). Briefly, the analysis derives a family of metrics that measure “distance” (i.e.,
199 dissimilarity) between spike trains. Each of these metrics represents the “cost” of transforming
200 one spike train into another by changing a different aspect of the spike trains that are being
201 compared. These include the number of spikes and the precise timing of spikes. The simplest of
202 this family of metrics represents the difference in the number of spikes contained in two spike
203 trains associated with two responses. To calculate cost in this case, each spike that is either
204 deleted or added incurs a cost of “1”, so that this metric, D^{count} , is simply the arithmetic
205 difference between the number of spikes in each response.

206 To measure the difference between two spike trains in terms of the arrangement of spikes
207 in time requires a definition of how close in time two spikes need to occur to be considered
208 equivalent. In the family of metrics described by Victor and Purpura (1996, 1997), the similarity

209 of the timing of spikes in two responses is calculated at a variety of levels of precision, measured
210 by a parameter called “ q .” The cost of adding or deleting a spike is set at “1” as in D^{count} and, in
211 addition, the cost of moving a spike by an amount of time t is set at qt where q is in units of
212 1/sec. The resulting metric for spike timing is called $D^{spike}[q]$. For each metric, the information
213 conveyed at various levels of precision (values of q) was calculated, and the value of q at which
214 information is maximized was obtained (see Di Lorenzo and Victor 2003; Victor and Purpura
215 1996, 1997). Thus, the relative contribution of spike count and spike timing to the information
216 conveyed by taste responses can be quantified.

217 Importantly, there are several additional analyses that serve as controls for the possibility
218 of spurious results. These are detailed in Victor and Purpura (1996, 1997). First, the values of H
219 calculated from observed responses were compared with the values of H calculated from a
220 dataset in which the observed responses were randomly assigned to the various clusters of
221 tastant. This served as a control for the statistical effects of a finite dataset and was called $H_{shuffle}$.
222 Second, to distinguish between the firing rate envelope (time course of response) and the precise
223 firing pattern, we applied metric space analysis to surrogate datasets created by randomly
224 exchanging spikes between individual responses belonging to the same tastant. These surrogate
225 datasets, called $H_{exchange}$, had post-stimulus time histograms that were identical to those of the
226 actual responses, with the identical number of spikes for each trial. If the value of H for the
227 actual response data was greater than the value of $H_{exchange}$ (mean \pm 2 SD), we concluded that the
228 information contributed by spike timing in individual trials was contributing to taste coding,
229 above and beyond that contributed by the rate envelope and spike count alone.

230

231 ***Histology***

232 At the end of each experiment, a lesion was produced through the recording electrode.
233 (0.1 mA DC for 5 sec) at the final recording site. The rat was then overdosed with urethane and
234 perfused transcardially with isotonic saline (0.15 M NaCl) and formol saline (10% formaldehyde
235 in isotonic saline). The brain was removed and processed for histological reconstruction of the
236 recording site(s). Frozen sections (80 μ m) were mounted on gelatinized slides and stained with
237 cresyl violet.

238

239

240
241**RESULTS**242 *General response characteristics*

243 Responses to exemplars of the four prototypical taste qualities were recorded from 44
244 PbN cells. Thirty-nine of 44 cells were tested with multiple trials of each stimulus (range = 2 to
245 26 trials; mean = 11.8 ± 1.13 ; median = 10). The average spontaneous rate across all cells was
246 3.9 ± 0.6 sps. When cells were categorized by the stimulus that evoked the highest magnitude of
247 response, 28 cells were NaCl best, 7 cells were HCl best, 5 cells were quinine best and 4 cells
248 were sucrose best. The average response magnitudes to the four taste stimuli (\pm SEM) were as
249 follows: sucrose, 5.65 ± 1.15 ; NaCl, 20.13 ± 2.47 ; HCl, 11.10 ± 1.70 , quinine, 10.74 ± 1.64 .
250 The mean breadth of tuning across taste stimuli as quantified by the Uncertainty measure was U
251 $= 0.78 \pm 0.02$ with a range of $U = 0.32$ to $U = 0.99$.

252 Variability in response magnitude with repeated presentations of a given stimulus was
253 assessed by calculating the coefficient of variation (CV; standard deviation/mean). The mean
254 CV across tastants in all cells was 0.45 ± 0.04 . Levels of variability across trials were similar for
255 all tastants tested: the CV for NaCl = 0.41 ± 0.07 , for HCl = 0.49 ± 0.09 , for quinine = $0.43 \pm$
256 0.06 and for sucrose = 0.49 ± 0.06 . A one-way ANOVA applied to these data showed no
257 significant effects of stimulus ($F_{3,123} = 0.31$, $P > 0.05$). Across cells and stimuli, the average CV
258 for the best stimulus of a cell (0.31 ± 0.04) was significantly smaller (Student's t test, $P < 0.01$)
259 than the average CV for non-best stimuli (CV = 0.54 ± 0.05). This reflected the fact that taste
260 stimuli that evoked higher response magnitudes showed relatively less variability across trials
261 than those that evoked smaller responses as evidenced by a significant negative correlation
262 between response magnitude and CV ($r = -0.49$, $P < 0.001$).

263

287 corresponds to $H=2$). The contribution of spike timing (information from spike timing is greater
 288 than that shown by the exchange-resampled control analyses) adds the remaining 0.16 bits for a
 289 total of 2.0 bits at q values between 8 and 16. In contrast, Figure 2A and B, right, shows the
 290 responses and information plot from a broadly tuned cell ($U = 0.90$) with a significant
 291 contribution of spike timing at q values between 4 and 32. This cell responded to all four taste
 292 stimuli. In this case, spike timing contributed 35% more information than spike count alone.

293 -----

294 Insert Figure 2 about here.

295 -----

296 The proportional contribution of temporal coding (including the contribution of the
 297 temporal envelope) was calculated with the following formula:

$$\frac{H_{\max} - H_{\text{count}}}{H_{\text{count}}}$$

298
 299 There was a significant positive correlation between the breadth of tuning of PbN cells and the
 300 proportional contribution of temporal coding such that cells that were broadly tuned showed
 301 greater information conveyed by temporal coding ($r = 0.51, P < 0.001$) (see Figure 3). Although
 302 it might appear that this significant correlation was driven by the contribution of four cells that
 303 are plotted above the rest, the relationship between breadth of tuning and temporal coding
 304 remains significant when the analysis is recalculated without those four cells ($r = 0.40, P < 0.05$).
 305 In contrast, there was no relationship between the best stimulus of a cell and the proportion of
 306 total information conveyed by temporal coding. Most cells were either N best ($n=20$) or H best
 307 ($N=6$) and a comparison between the proportion of information contributed by temporal coding
 308 for these two groups was not statistically significant ($P > 0.27$).

309 -----

310 Insert Figure 3 about here.

311 -----

312 *Comparison of temporal coding in the PbN and the NTS*

313 Data from the present study were compared with data collapsed from two previous
314 studies of temporal coding in the NTS (n = 32 cells total; Di Lorenzo and Victor 2003, 2007). In
315 general, results showed that taste responses in the PbN were more variable across trials than
316 those in the NTS but that measures of temporal coding in the PbN were not significantly
317 different than those in the NTS. Specifically, the average CV of taste responses in the PbN (0.45
318 ± 0.04) was significantly larger than the average CV of taste responses in the NTS ($CV = 0.32 \pm$
319 0.02 ; Student's t test, $P < 0.01$). However, the average total amount of information conveyed by
320 spike count and spike timing (H_{\max}) was similar across structures: 1.33 ± 0.09 among PbN cells
321 and 1.21 ± 0.08 in the NTS (Student's t test, $P > 0.3$). Figure 4A shows the values of H_{\max} in all
322 PbN and NTS cells, plotted as percentiles. Information conveyed by spike count alone (H_{count})
323 was also similar in the two structures: 0.94 ± 0.09 in PbN and 0.82 ± 0.06 . In Figure 4B, H_{count} is
324 plotted against H_{\max} to illustrate the relative contribution of spike timing to the total amount of
325 information. The dotted line in the diagonal shows the condition where spike timing does not
326 contribute any information to the total. In this plot it can be seen that PbN and NTS cells are
327 intermingled, suggesting that there is no difference between these two nuclei in the relative
328 contribution of spike timing to the total amount of information. In fact, the average proportion of
329 the total information contributed by spike timing was 0.81 ± 0.21 across PbN cells and $0.58 \pm$
330 0.09 across NTS cells. Although these values are different, the difference is not statistically
331 reliable (Student's t test, $p = 0.3$). Much of the difference can be explained by a few PbN cells
332 that show a very small H_{count} , so that even a relatively small H_{\max} will produce a very large

333 proportionate contribution of spike timing. The median values for this proportion were more
334 similar across structures (0.43 for the PbN and 0.53 for the NTS). Finally, the average level of
335 temporal precision at which information is at a maximum (q_{\max}) was 7.90 ± 1.45 in the PbN and
336 7.12 ± 0.99 in the NTS. Not surprisingly, the distribution of q_{\max} values across PbN and NTS
337 cells, plotted as percentiles, is nearly identical (Figure 4C). Collectively, these data show that
338 information conveyed by both spike count and spike timing is preserved as it is conveyed from
339 the NTS to the PbN, and further, that spike timing is significant at the same level of temporal
340 precision in both structures.

341 -----

342 Insert Figure 4 about here.

343 -----

344 *Histology*

345 Lesions corresponding to the locations of 21 of 29 cells analyzed for temporal coding
346 were confined within the PbN (see Figure 5). The lesions were largely concentrated in the
347 caudal PbN, located 9.8 mm caudal to bregma. The number of lesions decreased precipitously in
348 more rostral planes. Lesions were most often located on the dorsal and ventral borders of the
349 PbN, encompassing the ventrolateral, ventromedial, dorsal medial and central medial subnuclei.

350 -----

351 Insert Figure 5 about here.

352 -----

353

354
355**DISCUSSION**

356 Analyses of taste responses in single cells in the PbN showed that temporal coding
357 provided a significant advantage over rate coding in nearly every cell in spite of significant trial-
358 to-trial variability in response magnitude. In particular, spike timing contributed a significant
359 amount of information about taste quality above and beyond that contributed by spike count
360 alone in 48 % of the cells. In another 48% of the cells, the rate envelope of the response was
361 more informative than spike count. Comparison with previously published data recorded from
362 taste-responsive NTS cells (Di Lorenzo and Victor 2003, 2006) provided evidence that PbN cells
363 show significantly more trial-to-trial variability than NTS cells. Even so, the distribution,
364 amount and proportion of information contributed by the temporal features of taste responses
365 were similar to those observed in the PbN in the present study. The temporal precision with
366 which spike timing conveyed information was also similar in NTS and PbN. Further, results
367 showed that broadly tuned PbN cells, like those in the NTS (Di Lorenzo and Victor 2003; Di
368 Lorenzo et al. 2009), generally encode more information using spike timing than cells that are
369 narrowly tuned. Altogether, these data imply that PbN cells use the temporal features of taste-
370 evoked spike trains to convey information about taste quality and that this information is
371 transmitted from the NTS to the PbN with high fidelity, even in the face of an increase in trial-to-
372 trial variability in response magnitude.

373 The widespread incidence of temporal coding among PbN cells reported here points to
374 the temporal features of taste responses in this region as an informative, but relatively neglected,
375 aspect of taste responses. While the presence of temporal coding has been well documented in
376 the NTS (Di Lorenzo and Victor 2003; Roussin et al. 2008), few reports have touched on this
377 issue in the PbN, and none have quantified the information contributed by temporal coding.

378 Early on, Perrotto and Scott (1976) and Scott and Perrotto (1980) described taste quality-specific
379 time courses (rate envelopes) of the average peristimulus-time histogram (PSTH) of PbN
380 responses. Perrotto and Scott (1976) also noted that the ratio of the magnitude of the phasic
381 component of the response (usually the number of spike in the second 100 msec time bin of the
382 PSTH) to the later tonic component (number of spikes in 0.3-1.3 sec of the PSTH) of the
383 response varied systematically according to taste quality. More detailed analyses of taste
384 responses in the rabbit PbN using principal components analyses of the normalized responses,
385 however, suggested that only the hedonic valence (pleasant or unpleasant) of a tastant could be
386 signaled by the time course of response (Di Lorenzo and Schwartzbaum 1982). By examining
387 the fine temporal characteristics of spike trains, the present data further suggest that the time
388 course of response can also convey information about taste quality in about half of the
389 population of PbN cells. Later, Erickson et al. (1994) used a fuzzy set approach to derive
390 prototypical time courses from PSTHs across cells. Each taste response was then assigned a
391 “loading” that measured the association of that response with each of the prototypical time
392 courses. Using this method, the time courses of each cell’s response could be accurately
393 reconstructed. From these data, Erickson et al. (1994) speculated that the prototypical time
394 courses originated in the receptor and that the actual time course of any given response was the
395 result of the convergence of inputs originating from different receptor processes. In effect, the
396 argument was that the time course of response was not a function of the cell, but of the
397 interaction of various peripherally derived processes. While this idea is not at all inconsistent
398 with the present data, we show that spike timing, as well as the time course of response can be
399 used to distinguish among tastants of different qualities.

400 Although the present report highlights the similarities in the quantitative aspects of
401 temporal coding in NTS and PbN, there is ample reason to suspect that this information may be
402 used in different ways. That is, the PbN is thought to be involved in conditioned taste-visceral
403 associations while the NTS may be more concerned with unconditioned taste-evoked ingestion
404 and behavioral taste reactivity (reviewed in Lundy 2008). In the NTS, lick-contingent electrical
405 stimulation with temporal patterns of pulses that mimic actual electrophysiological responses to
406 particular taste qualities can evoke specific and predictable taste sensations in rats (Di Lorenzo
407 and Hecht 1993; Di Lorenzo et al. 2003, 2009b), observations that underscore the functionality
408 of temporal coding in the NTS. Given the different function of the PbN, it is an open question as
409 to whether the same type of stimulation in the PbN would produce similar effects. On the other
410 hand, PbN/NTS projections may allow information conveyed by temporal coding in the PbN to
411 amplify the signal conveyed by spike timing in the NTS. In this context, it is worth noting that
412 there are projections from the PbN to ventral subnucleus of the NTS (Karimnamazi and Travers
413 1998), an area that then projects to oromotor nuclei in the reticular formation (Halsell et al. 1996)
414 where spike timing may be critical to the selection of appropriate oromotor behaviors
415 (Venugopal et al. 2010).

416

417 ***Trial-to-trial variability***

418 Considered in the context of data from the chorda tympani nerve (CT: a branch of the
419 facial nerve that innervates taste buds on the rostral 2/3 of the tongue; Ogawa et al. 1973) and the
420 NTS (Di Lorenzo and Victor 2003, 2007), present data from the PbN extends a trend of
421 increasing trial-to-trial variability from peripheral to central structures along the gustatory
422 neuraxis. In a study of trial-to-trial variability of taste responses recorded from CT fibers, for

423 example, Ogawa et al. (1973) reported that the average CV ranged between 0.1 and 0.25. The
424 mean CV of CT fibers as calculated from Table 1 of Ogawa et al. (1973) was 0.19 ± 0.02 . This
425 value was significantly lower than the average CV across NTS cells (0.32 ± 0.02 , Student's *t* test,
426 $P < 0.01$). In turn, the average CV across PbN cells (0.44 ± 0.03) was significantly greater than
427 that in the NTS (Student's *t* test, $P < 0.01$).

428 Escalating trial-to-trial variability in the central gustatory pathway may be due to
429 increasing complexity in the network of interconnections as the sensory signal ascends through
430 the brain. That is, as the signal is transmitted from structure to structure, there are more and
431 more loops of information that can influence responding of single cells and/or ensembles (see
432 Jones et al. 2007) Related to this point, Fontanini and Katz (2008) cited evidence from a number
433 of sensory systems and neural structures to argue that trial-to-trial variability may be an essential
434 feature of normal sensory processing. That is, they maintained that, rather than reflecting noise in
435 the system, this type of variability may be an expression a naturally fluctuating state of the neural
436 network. These fluctuations can reflect variables such as attention (Fontanini and Katz 2006) or
437 context (Di Lorenzo et al. 2003b) for example. In their work on the gustatory cortex, Katz and
438 colleagues (Jones et al. 2007; Fontanini and Katz 2006, 2008) have shown that ensembles of
439 cortical cells traverse through stimulus-specific stereotypic sequences of states (defined as
440 coordinated firing rates across cells) when taste stimuli are presented. From trial-to-trial,
441 however, the length of time that the network remains in each state may expand or contract, but
442 the sequence remains the same. Such network dynamics may also be present in the PbN cells
443 considering the rich network of intra- and extra-nuclear connections (Cho et al. 2003; Li et al.
444 2005; Di Lorenzo and Monroe 1992; 1995).

445

446 *Conservation of information conveyed by temporal coding in the PbN*

447 In spite of a significant increase in trial-to-trial variability in response magnitude, present
448 data show that the information conveyed by spike timing is conserved as it is passed from NTS
449 to PbN. Of course, the overall similarity in the prevalence and precision of temporal coding
450 between these two structures does not directly imply that the PbN merely mirrors the spike
451 patterns relayed from the NTS. However, in a study of simultaneously recorded pairs of taste-
452 responsive cells, one from the NTS and the other from the PbN, we showed that PbN cells that
453 were functionally connected to NTS cells did indeed follow the activity of NTS cells spike by
454 spike in a roughly damped oscillatory pattern for the first three sec of the response (Di Lorenzo
455 and Monroe 1997; Di Lorenzo et al. 2009c). As the drive from the NTS cells diminishes, the
456 responses from the PbN, though still robust, become increasingly independent from those in the
457 NTS. Since our analyses of taste responses focused on the initial two sec of response, it is
458 possible that information conveyed by spike timing in PbN cells was transmitted directly from
459 relay cells in the NTS. That would be consistent with the observation that the amount of
460 information conveyed by spike timing and the temporal precision with which the information
461 was conveyed were identical in NTS and PbN cells. In addition, taste-responsive PbN cells that
462 used temporal coding were located in the central medial and ventral lateral regions of the PbN,
463 an area that receives dense synaptic input from the NTS (Herbert et al. 1990; Halsell and Travers
464 1997).

465 It can also be hypothesized that the conservation of information through temporal coding
466 as it is transferred from the NTS to the PbN may be the result of a common descending drive
467 from forebrain structures such as the lateral hypothalamus (LH; Li et al. 2005; Cho et al. 2003),
468 bed nucleus of the stria terminalis (BNST; Li and Cho 2006), central nucleus of the amygdala

469 (CeA; Cho et al. 2003; Li et al. 2005) and gustatory cortex (GC; Di Lorenzo and Monroe 1992;
470 1995). However, although both NTS and PbN receive input from the same structures, the
471 character (excitatory or inhibitory) and selectivity of the influences can differ (reviewed in
472 Lundy 2008). Moreover, the proportion of cells in each of these structures that projects to both
473 the NTS and PbN is < 20% (Kang and Lundy 2009) supporting the idea that the NTS and PbN
474 receive differential modulatory influences. It is therefore unlikely that centrifugal feedback is
475 responsible for similarities with respect to temporal coding of tastants in NTS and PbN cells.

476

477 ***Conclusions***

478 In the present study, spike timing in taste-responsive PbN cells was found to significantly
479 contribute information about taste quality in about half of the sample, with broadly tuned PbN
480 cells conveying proportionately more information than narrowly tuned cells. The fraction of the
481 total amount of information conveyed by temporal coding in the PbN and the temporal precision
482 at which information from temporal coding was maximized was identical to that in the NTS,
483 even though trial-to-trial variability was higher in the PbN than in the NTS. In all, these data
484 show that the neural representation of taste stimuli through the temporal characteristics of the
485 taste-evoked spike trains is strikingly similar in both PbN and NTS, suggesting a high fidelity of
486 synaptic transmission from one structure to the other. Although there is evidence that the
487 temporal characteristics of taste responses can be “read” by cells in the NTS (Di Lorenzo and
488 Hecht 1993; Di Lorenzo et al. 2003, 2009b), a corresponding demonstration that the same
489 applies to the PbN awaits further experimentation.

490

491

492
493

ACKNOWLEDGEMENTS

494 The authors wish to acknowledge the substantial technical contribution of Daniel Platt.

495 Histological processing of tissue was done by Obeda Lavin, for which we are also grateful.

496

497 PMD was supported by NIDCD grant RO1DC006914. JV was supported in part by

498 MH68012, “Algorithms and Informatics for Analysis of Neural Coding” (PI D. Gardner).

499

500
501
502
503
504
505
506
507
508
509
510
511
512
513
514
515
516
517
518
519
520
521
522

REFERENCES

Chen, J-Y, Victor, JD, Di Lorenzo, PM. Temporal coding of intensity of NaCl and HCl in the nucleus of the solitary tract of the rat. *J Neurophysiol* in press

Cho YK, Li CS, Smith DV. Descending influences from the lateral hypothalamus and amygdala converge onto medullary taste neurons. *Chem Senses* 28(2): 155-171, 2003.

Di Lorenzo PM, Monroe S. Corticofugal input to taste-responsive units in the parabrachial pons. *Brain Res Bull* 29(6): 925-930, 1992.

Di Lorenzo PM, Monroe S. Corticofugal influence on taste responses in the nucleus of the solitary tract in the rat. *J Neurophysiol* 74(1): 258-272, 1995.

Di Lorenzo PM, Hecht GS. Perceptual consequences of electrical stimulation in the gustatory system. *Behav Neurosci* 107(1): 130-138, 1993.

Di Lorenzo PM, Monroe S. Transfer of information about taste from the nucleus of the solitary tract to the parabrachial nucleus of the pons. *Brain Res* 763; 167-181, 1997.

Di Lorenzo PM, Hallock RM, Kennedy DP. Temporal coding of sensation: mimicking taste quality with electrical stimulation of the brain. *Behav Neurosci* 117(6): 1423-1433, 2003.

- 523 **Di Lorenzo PM, Lemon CH, Reich CG.** Dynamic coding of taste stimuli in the brainstem:
524 effects of brief pulse of taste stimuli on subsequent taste responses. *J Neurosci* 23(26): 8893-
525 8902, 2003b.
- 526
- 527 **Di Lorenzo PM, Schwartzbaum JS.** Coding of gustatory information in the pontine
528 parabrachial nuclei of the rabbit: Temporal patterns of neural response. *Brain Res* 251: 245-
529 257, 1982
- 530
- 531 **Di Lorenzo PM, Victor JD.** Taste response variability and temporal coding in the nucleus of the
532 solitary tract of the rat. *J Neurophysiol* 90(3): 1418-31, 2003.
- 533
- 534 **Di Lorenzo PM, Victor JD.** Neural coding mechanisms for flow rate in taste-responsive cells in
535 the nucleus of the solitary tract of the rat. *J Neurophysiol* 97(2): 1857-1861, 2007.
- 536
- 537 **Di Lorenzo PM, Chen JY, Victor JD.** Quality time: representation of a multimodal sensory
538 domain through temporal coding. *J Neurosci* 29(29): 9227-9238, 2009.
- 539
- 540 **Di Lorenzo PM, Leshchinskiy S, Moroney DN, Ozdoba JM.** Making time count: functional
541 evidence for temporal coding of taste sensation. *Behav Neurosci* 123(1): 14-25, 2009b.
- 542
- 543 **Di Lorenzo PM, Platt D, Victor JD.** Information processing in the parabrachial nucleus of the
544 pons. *Ann N Y Acad Sci* 1170: 365-371, 2009c.
- 545

- 546 **Erickson RP, Di Lorenzo PM, Woodbury MA.** Classification of taste responses in brain stem:
547 membership in fuzzy sets. *J Neurophysiol* 71(6): 2139-2150, 1994.
548
- 549 **Fontanini A, Katz DB.** State-dependent modulation of time-varying gustatory responses. *J*
550 *Neurophysiol* 96(6): 3183-3193, 2006.
551
- 552 **Fontanini A, Katz DB.** Behavioral states, network states, and sensory response variability. *J*
553 *Neurophysiol* 100(3), 1160-1168, 2008.
554
- 555 **Herbert H, Moga HM, Saper CB.** Connections of the parabrachial nucleus of the solitary tract
556 and the medullary reticular formation in the rat. *J Comp Neurol* 293: 540-580, 1990.
557
- 558 **Halsell CB, Travers SP, Travers JB.** Ascending and descending projections from the rostral
559 nucleus of the solitary tract originate from separate neuronal populations. *Neuroscience* 72(1):
560 185-97, 1996.
561
- 562 **Halsell CB, Travers SP.** Anterior and posterior oral cavity responsive neurons are differentially
563 distributed among parabrachial subnuclei in rat. *J Neurophysiol* 78: 920-938, 1997.
564
- 565 **Jones LM, Fontanini A, Sadacca BF, Miller P, Katz DB.** Natural stimuli evoke dynamic
566 sequences of states in sensory cortical ensembles. *Proc Natl Acad Sci U S A* 104(47): 18772-
567 18777, 2007.
568

- 569 **Kang Y, Lundy RF.** Terminal field specificity of forebrain efferent axons to brainstem
570 gustatory nuclei. *Brain Res* 1248: 76-85, 2009.
571
- 572 **Karimnamazi H, Travers JB.** Differential projections from the gustatory responsive
573 parabrachial regions to the medulla and forebrain. *Brain Res* 813: 283-302, 1998.
574
- 575 **Katz DB, Nicolelis MA, Simon SA.** Gustatory processing is dynamic and distributed. *Curr Opin*
576 *Neurobiol* 12(4): 448-454, 2002.
577
- 578 **Li CS, Cho YK, Smith DV.** Modulation of parabrachial taste neurons by electrical and chemical
579 stimulation of the lateral hypothalamus and amygdala. *J Neurophysiol* 93(3): 1183-1196,
580 2005.
581
- 582 **Li CS, Cho YK.** Efferent projection from the bed nucleus of the stria terminalis suppresses
583 activity of taste-responsive neurons in the hamster parabrachial nuclei. *Am J Physiol Regul*
584 *Integr Comp Physiol* 291(4): R914-R926, 2006.
585
- 586 **Lundy RF Jr, Norgren R.** Activity in the hypothalamus, amygdala and cortex generates
587 bilateral and convergent modulation of pontine gustatory neurons. *J Neurophysiol* 91: 1143-
588 1157, 2004.
589
- 590 **Lundy RF Jr.** Gustatory hedonic value: potential function for forebrain control of brainstem
591 taste processing. *Neurosci Biobehav Rev* 32(8): 1601-1606, 2008.

- 592
- 593 **Norgren R.** Projections from the nucleus of the solitary tract in the rat. *Neuroscience* 3(2): 207-
- 594 218, 1978.
- 595
- 596 **Ogawa H, Sato M, Yamashita S.** Variability in impulse discharges in rat chorda tympani fibers
- 597 in response to repeated gustatory stimulations. *Physiol Behav* 11(4): 469-479, 1973.
- 598
- 599 **Perrotto RS, Scott TR.** Gustatory neural coding in the pons. *Brain Res* 110(2): 283-300, 1976
- 600 **Roussin AT, Victor JD, Chen JY, Di Lorenzo PM.** Variability in responses and temporal
- 601 coding of tastants of similar quality in the nucleus of the solitary tract of the rat. *J*
- 602 *Neurophysiol* 99: 644–655, 2008.
- 603
- 604 **Simon SA, de Araujo IE, Gutierrez R, Nicolelis MA.** The neural mechanisms of gustation: a
- 605 distributed processing code. *Nat Rev Neurosci* 7(11): 890-901, 2006.
- 606
- 607 **Smith DV, Travers JB.** A metric for the breadth of tuning of gustatory neurons. *Chem Senses*
- 608 (4): 215-229, 1979.
- 609
- 610 **Travers JB.** Efferent projections from the anterior nucleus of the solitary tract of the hamster.
- 611 *Brain Res* 457(1): 1-11, 1988.
- 612
- 613 **Travers JB, Norgren R.** Afferent projections to the oral motor nuclei in the rat. *J Comp Neurol*
- 614 22(3): 280-298, 1983.

615

616 **Venugopal S, Boulant JA, Chen Z, Travers JB.** Intrinsic membrane properties of pre-oromotor
617 neurons in the intermediate zone of the medullary reticular formation. *Neuroscience* 168(1):
618 21-47, 2010.

619

620 **Victor JD, Purpura KP.** Nature and precision of temporal coding in visual cortex: a metric
621 space analysis. *J Neurophysiol* 76(2): 1310-1326, 1996.

622

623 **Victor JD, Purpura KP.** Sensory coding in cortical neurons. Recent results and speculations.
624 *Ann N Y Acad Sci* 835: 330-352, 1997.

625

626 **Whitehead MC.** Neuronal architecture of the nucleus of the solitary tract in the hamster. *J Comp*
627 *Neurol* 276(4): 547-572, 1988.

628

629

630

631

632
633

FIGURE LEGENDS

634

635 **Figure 1.** Plot of the amount of information (in bits) contributed by spike count alone (H_o) vs.
636 the maximum amount of information contributed by spike count plus the temporal features of the
637 response (H_{\max}). Filled squares indicate cells with responses that showed a significant
638 contribution of spike timing, i.e. $H_{\max} > H_{\text{exchange}} + 2\text{SD}$.

639

640 **Figure 2.** Taste responses and results of temporal coding analyses in a relatively narrowly tuned
641 and a broadly tuned PbN cell. A. Raw data showing responses to the basic taste qualities in a
642 relatively narrowly tuned cell (Cell A) and a broadly tuned cell (Cell B). B. Information plots
643 associated with Cells A and B shown in A. In both cells, spike timing contributes significantly
644 more information about taste quality than either spike count alone, as indicated by the value of
645 the plot of the information from actual responses at $q = 0$, or the rate envelope of response, as
646 indicated by the plot of the exchange resampled data. However, in Cell A, spike count alone
647 contributes nearly all of the information necessary to discriminate among four tastants (2.0 bits).

648

649 **Figure 3.** Plot of the Uncertainty measure (U , breadth of tuning) vs. the proportion of
650 information that was conveyed by the temporal features of the response ($(H_{\max} - H_{\text{count}}) / H_{\text{count}}$). Line
651 on plot shows result of linear regression.

652

653 **Figure 4.** Comparison of temporal coding in the PbN and NTS. A. Graph of H_{\max} in all PbN
654 and NTS cells, plotted as percentiles. B. Plot of the amount of information (in bits) contributed
655 by spike count alone (H_o) vs. the maximum amount of information contributed by spike count

656 plus the temporal features of the response (H_{\max}) for PbN cells (filled circles) and NTS cells
657 (open squares). C. Distribution of values of q_{\max} (a measure of temporal precision) at which
658 information is at a maximum value (H_{\max}), plotted as percentiles.

659

660 **Figure 5.** Histological results showing recording site for 21 cells. Left, line drawings of coronal
661 sections at various AP levels through the PbN. Numbers in lower right of each drawing indicate
662 distance in mm caudal to bregma. Line in lower right of bottom drawing indicates 0.5 mm.

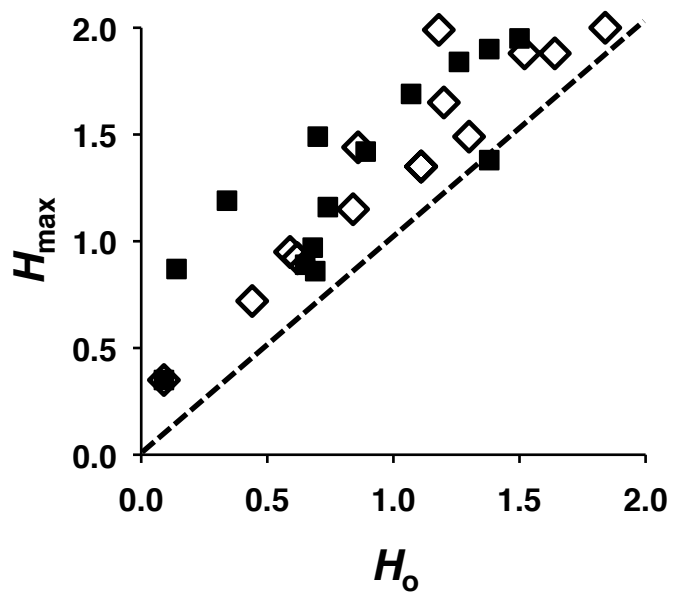
663 Abbreviations are as follows: DM, dorsomedial n.; CM, central medial n.; VM, ventromedial n.;
664 VL, ventral lateral n.; CL, central lateral n.; ELo, external lateral outer n.; external lateral inner n.

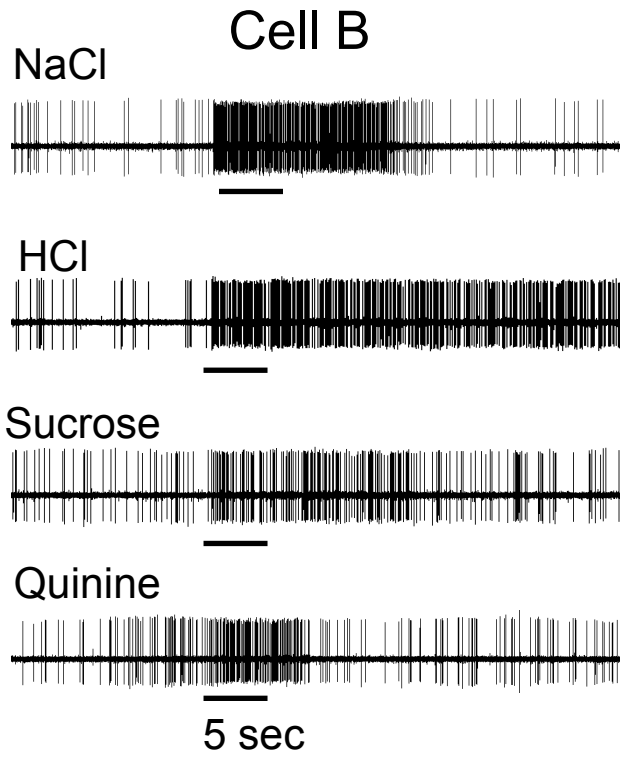
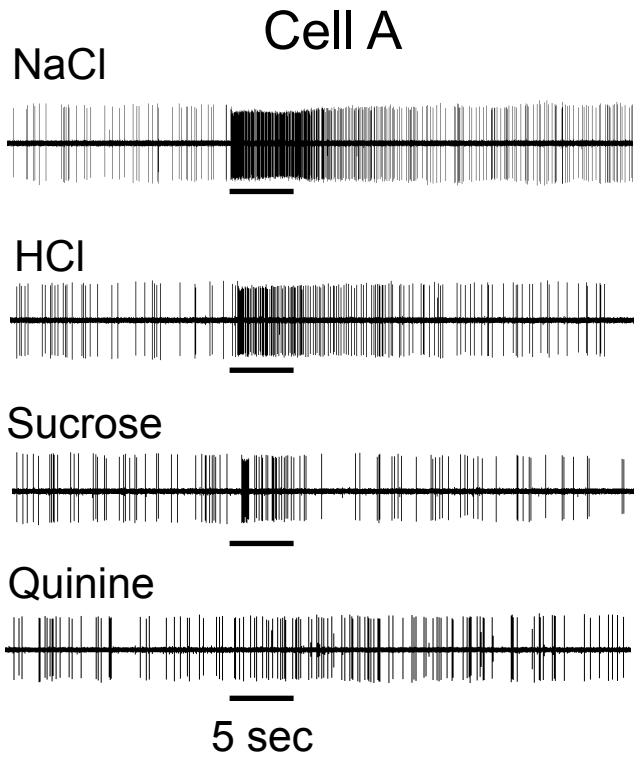
665 Right, photomicrographs of coronal sections showing lesions (asterisks in figure) marking
666 recording sites at AP levels corresponding to the line drawings to the left.

667

■ $H_{\max} > H_{\text{exchange}} + 2\text{SD}$

◇ $H_{\max} < H_{\text{exchange}} + 2\text{SD}$



A**B**

— Information from actual responses
— Exchange resampled $\pm 2SD$
— Shuffled data $\pm 2SD$

